Ground-State Proton Transfer Tautomer of Al(III)−Salicylate Complexes in Ethanol Solution

Z. Wang,* D. M. Friedrich,† C. C. Ainsworth, S. L. Hemmer, A. G. Joly, and M. R. Beversluis‡

Pacific Northwest National Laboratory, Richland, Washington 99352

Received: August 4, 2000; In Final Form: November 15, 2000

The tautomerization of salicylate anion in the presence of Al(III) in ethanol was studied by UV−visible absorption spectroscopy and fluorescence spectroscopy, anisotropy, and lifetime measurements from 100 to 298 K. Complexation with Al(III) causes an equilibrium shift from the normal form of the salicylate anion toward the tautomer form, demonstrating that the presence of a highly charged cation, Al(III), stabilizes the tautomer form of salicylate. Spectra and fluorescence lifetimes of salicylate and other salicyl derivatives in the presence of Al(III) reveal three types of Al(III)−salicylate complexes. In type I complexes, salicylate binds to Al(III) through the carboxylate group, preserving the intramolecular hydrogen bond between the carbonyl oxygen and the phenol group, as indicated by the largely Stokes-shifted fluorescence emission following an excited state proton transfer process. In type II complexes, salicylate binds to Al(III) through the carboxylate group, but the phenol proton is oriented away from the carbonyl oxygen so that the complex shows short wavelength fluorescence emission characteristic of substituted phenolic compounds. In type III complexes, Al(III) stabilizes and binds to the tautomer form of salicylate through the phenolate oxygen, in which salicylate exists in its proton transferred tautomer form. Absorption spectra recorded at temperatures between 100 K anf 298 K indicate that the type III tautomer complex is energetically favored at low temperature, although type I is the dominant species at room temperature. All three types of complexes are interconvertible above the ethanol glass transition temperature. However, below the glass transition temperature interconversion ceases, indicating large amplitude atomic motion is involved in the conversion.

I. Introduction

Methylsalicylate and its derivatives (MSD) show two fluorescence emission bands, one in the UV region and the other in the blue region.[1−12] It has been accepted that the two different emissions are from different rotamers of these molecules. The largely Stokes-shifted blue emission is due to the presence of an intramolecular hydrogen bond (IHB) between the phenol group and the carbonyl oxygen of the carboxyl group (Figure 1 structure **A1**). Molecules existing in this form are often referred to as "closed form I". In the excited electronic state the charge density at the phenol oxygen is decreased while that of the carbonyl oxygen is increased, and consequently the phenol proton transfers to the carbonyl oxygen (**A4**). Such a process is called excited-state intramolecular proton transfer (ESIPT), and the proton-transferred species is termed the "tautomer" to distinguish it from the "normal" IHB form.[13−15] The excited state of the tautomer is energetically stabilized relative to the excited state of the normal form, resulting in a red-shift of the fluorescence emission from the UV (normal form emission) to the visible (ESIPT or tautomer form emission). For MSDs the proton-transfer process is believed to be barrierless on the excited-state potential energy surface.[16−20] Both pump−probe and isotope substitution experiments indicate that the proton transfer process is complete in less than one picosecond, which is beyond the resolution limit of the previously utilized fluorescence techniques.[21,22]

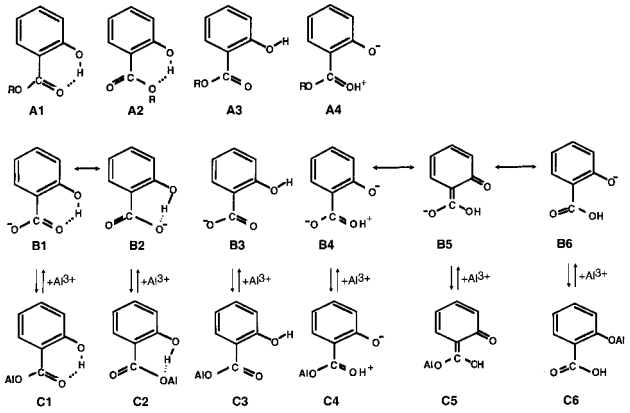

Figure 1. Structures of methyl salicylate derivatives.

The UV-emitting species of MSDs are assigned to a rotameric isomer (rotomer) in which the phenol proton is not hydrogen-bonded to the carbonyl oxygen.[23] For methylsalicylate and salicylic acid, the phenol proton may be hydrogen-bonded either to the carboxyl oxygen of the methoxy or to the acid group (**A2**), often referred to as "closed form II". For MSDs that lack a carboxyl oxygen such as salicyl aldehyde, salicyl acetophenone, and salicyl amide (**A3**), the phenol proton is rotated away from the carbonyl group.[23−29] Molecules of this form are called "open form". Experimental observation of the open forms of methylsalicylate and salicylic acid have been reported.[23−25] The relative population of the hydrogen-bonded and the non-

* Author to whom correspondence should be addressed.
† Current address: OCLI/JDS Uniphase, 2789 Northpoint Parkway, Santa Rosa, CA 95407-7397. E-mail: dfriedrich@ocli.com.
‡ Current address: Department of Optics, University of Rochester, Rochester, NY 14627.

10.1021/jp002844a CCC: $20.00 © 2001 American Chemical Society
Published on Web 01/16/2001

hydrogen-bonded forms are dependent on the polarity and the hydrogen-bonding properties of the solvent.[30]

In the salicylate anion, the delocalized negative charge on the carboxylate group greatly stabilizes the hydrogen-bond between the phenol group and the carboxlate group. Consequently, the dissociation constant of the phenolic proton of the salicylate anion is extremely low ($pK_{a2} = 13.5$) compared with other phenol derivatives ($pK_a \sim 10$). Aqueous salicylate anion exists exclusively in the normal IHB form. Since the negative charge on the salicylate anion is delocalized, this corresponds to both structures **B1** and **B2** in Figure 1. No evidence for the open form (**B3**) exists in aqueous solutions. We recently reported observation of the proton-transferred tautomer of salicylate anion (resonance structures **B4**−**B6**), in polar aprotic solvents at room temperature.[30] The conversion reaction of the salicylate anion from the normal phenolic form (**B1**) to the tautomer form (**B4**−**B6**), N ↔ T, has an enthalpy change of $\Delta H = 1.6$ kcal mol^{-1} and an entropy change of $\Delta S = 0.97$ cal mol^{-1}. At 298 K the concentration equilibrium constant for [T]/[N] is 0.11.[30] The small enthalpy and entropy changes disfavor the formation of the tautomer at lower temperatures but enable detectable concentrations of the tautomer at room temperature. The tautomer has an absorption maximum at 325 nm which is 29 nm red-shifted relative to the normal phenolic form. Excitation of either form yields the same fluorescence emission spectra with an emission maximum at 415 nm, while the quantum yield of the tautomer is about 60% larger than the normal form. Both forms have identical fluorescence lifetimes, confirming that the proton-transfer process is much faster than the relaxation of the excited state. The tautomer is hypothesized as a metastable species for MSDs.

Aluminum is the most abundant metal element in the earth's crust. The interaction between aluminum and organic acids such as humic acid, biochemicals, and fertilizers has been shown to be important for many chemical, geochemical, plant toxicological, weathering, and mineral formation processes.[31−34] Essential to understanding such interactions are the speciation and bonding properties between Al(III), the most stable form of aluminum in nature, and the organic acid.[35−39] Several methods, including potentiometry,[40−42] ion exchange,[43,44] IR,[45−47] and ^{27}Al NMR,[48−50] have been used to characterize the Al(III)−organic acid complexes.

Theoretical electronic structure calculations of Al(III)−salicylate complexes comparing the bonding between Al(III) and the carboxylate oxygen and phenolate oxygen are not available. However, from a study of complexation between Al(III) and a series of hydroxycarboxylic acids, Motekaitis and Martell found that Al(III) has a very strong tendency toward displacement of protons from the hydroxyl groups of hydroxy acids.[51] They concluded from the thermodynamic stability constants of Al(III) complexes with catechol, tartaric acid, citric acid, phthalic acid, etc., that Al(III) binding with the hydroxyl oxygen is thermodynamically more stable than binding to the carboxylate oxygen. This follows the trend of the basicity of these oxygens. This general conclusion is consistent with the spectroscopic observations reported here for Al(III)−salicylate complexes.

The existence of both the normal and tautomer form of salicylate exposes several distinctive monodentate and bidentate binding sites such as the carboxylate group, the phenoxy group, and the methoxy group of the quinoidal form of the tautomer. This rich variety of binding and consequent effects on fluorescence provide a unique probe for the characterization of complexation between Al(III) and hydroxycarboxylic acids.

In this paper we report the results of a spectroscopic study of Al(III) complexation with salicylate in ethanol solutions. From the variations of the absorption spectra at different temperatures, fluorescence excitation and emission spectra, steady-state fluorescence anisotropies, and emission lifetimes, it is concluded that Al(III) forms three types of monodentate complexes with salicylate in ethanol. In type I, Al(III) binds to salicylate at the carboxylate oxygen preserving the intramolecular hydrogen-bond between the phenol group and the carbonyl group and thus displaying ESIPT-type fluorescence emission. In type II, Al(III) binds to the carboxylate group but in the open form. In type III, Al(III) binds to the phenolate oxygen of the proton-transferred tautomer of salicylate. Changes of the absorption spectra in the temperature range from 298 to 105 K indicate that the tautomer form of the Al(III)−salicylate complex (type III) is energetically favored relative to the normal form complex at lowered temperatures.

II. Experimental Section

Materials. Sodium salicylate, reagent grade, was purchased from Mallinckrodt Chemical Co. Anhydrous aluminum chloride (99.99%), lanthanum chloride (99.9%), anisic acid (2-methoxybenzoic acid, 99%), methyl salicylate (99.9+%), and anhydrous denatured ethanol, stored in a septum bottle, were purchased from Aldrich. Sodium hydroxide (0.1 M aqueous), HPCE grade, was purchased from Hewlett-Packard; 1.0 M hydrochloric acid in water, volumetric standard, was purchased from Aldrich. All chemicals were used as received without further purification. Solutions of 1×10^{-4} M of sodium salicylate and aluminum chloride in ethanol were prepared by weighing each compound and immediately transferring them into a glass solvent tube sealed with a Teflon-lined cap. The tube was opened only when the solution was transferred to a UV-quartz spectroscopic cell. Solvent transfer from the original bottle was performed under the protection of dried N_2 using Teflon syringes. Aqueous solutions of the acids and methylsalicylate were prepared using spectroscopic grade water from a Millipore reversed osmosis and ion exchange system, with ultraviolet sterilization of the finished water.

UV−visible absorption spectra were measured on a Cary III spectrometer with 1 cm pathlength quartz spectrophotometric cells. For absorption spectra recorded at temperatures lower than 298 K, the volume change of the solution due to the thermal expansion/contraction was corrected by normalizing the area at lower temperatures to that at 298 K assuming a constant total oscillator strength of species at different temperatures. This approach results in a distinct isosbestic point which validates such a treatment. Fluorescence excitation and emission spectra were taken on a SPEX Fluorolog II fluorimeter equipped with two double monochromators (SPEX1681), a 450 W xenon lamp, and a cooled photomultiplier tube detector. The monochromators of the fluorimeter were calibrated using mercury lines.

For experiments at temperatures lower than room temperature, a Cryo-Industries of American RC 152 cryogenic workstation equipped with a Lakeshore 330 autotuning temperature controller was used. With this apparatus, liquid N_2 was evaporated to cool the sample housed inside the copper block sample holder. The temperature of the nitrogen gas was controlled by an internal heater. Gas phase cooling of the sample allowed the temperature to be accurately adjusted to within ±0.01 °C. The cryogenic workstation was equipped with four Suprasil quartz windows which allow both absorption and fluorescence measurements to be performed at the desired temperature.

For the steady-state fluorescence anisotropy measurements, Glan-Thompson polarizers were placed in the light paths on

both the excitation side and the emission side immediately adjacent to the sample cell. On the emission side, a polarization scrambler was placed after the polarizer to minimize polarization bias of the emission monochromator.

The steady-state anisotropy at each wavelength, $R(\lambda)$, was calculated using eq 1:

$$R(\lambda)=[I_v(\lambda) - G(\lambda)\bullet I_h(\lambda)]/[I_v(\lambda) + 2\bullet G(\lambda)\bullet I_h(\lambda)] \quad (1)$$

where subscripts v and h refer to vertical and horizontal emission, respectively, when the excitation beam was vertically polarized. $G(\lambda)$ is the instrumental anisotropy bias factor for the sample given by eq 2:

$$G(\lambda) = I_{hv}(\lambda)/I_{hh}(\lambda) \quad (2)$$

where the first subscript, h, refers to horizontally polarized excitation light. The $G(\lambda)$ factor was further confirmed using anthracene in ethanol and a solvent mixture of 3-methylpentane and cyclohexane, for which the polarization anisotropy has been accurately measured previously.[52] Observations with crossed polarizers showed that birefringence depolarization was negligible in the measured samples and for salicylate solution in ethanol there is no optical activity.

Fluorescence lifetime measurements were carried out on a conventional time-correlated single photon counting apparatus.[53] Fluorescence lifetime analysis was calculated by fitting the experimental decay curves convoluted with the instrument function using a program written in this laboratory.[53] Laser excitation was provided by the frequency-doubled output of a cavity-dumped Coherent 702 dye laser operating between 580 and 610 nm or a Coherent Satori 774 dye laser operating between 620 and 683 nm. The dye lasers were pumped by the second harmonic of a mode-locked Coherent Antares Nd:YAG laser operating at 76 MHz. The fluorescence emission was collected with a pair of parabolic mirrors and focused into an American Holographic double monochromator. The dispersed light was detected by a microchannel plate photomultiplier. The laser pulse width was less than fifteen picoseconds and the measured instrument response was typically between 30 and 40 ps fwhm with the resolution limited by the electronics system. For each set of data, the decay curve has a peak intensity of $\geq 10^4$ counts. The spectral deconvolution of the absorption spectra was carried out using a commercial procedure in WaveMetrics IGOR assuming Gaussian spectral profiles.

III. Results and Discussion

UV−Visible Absorption Spectra. The absorption spectrum of 2.4×10^{-4} M sodium salicylate in ethanol solution at room temperature is shown in Figure 2a. The absorption maximum is located at 297 nm, which is similar to that of sodium salicylate in water, but the spectrum displays a more profound shoulder at longer wavelength (~340 nm). Due to the relatively weak intensity, precise deconvolution of the shoulder band from the main absorption band is problematic. However, from previous results in acetonitrile, it is known that the shoulder band is located around 325 nm.[30] The band at 297 nm corresponds to the normal form of the salicylate anion (**B1**) while the longer wavelength band corresponds to the proton-transferred tautomer of the salicylate anion (**B4**−**B6**).

Addition of $AlCl_3$ into sodium salicylate solution in ethanol causes both a red-shift of the absorption bands and a significant increase of the intensity of the shoulder band (Figure 2b). Assuming a Gaussian profile for the spectrum of the shoulder band, deconvolution of the absorption spectrum shows two

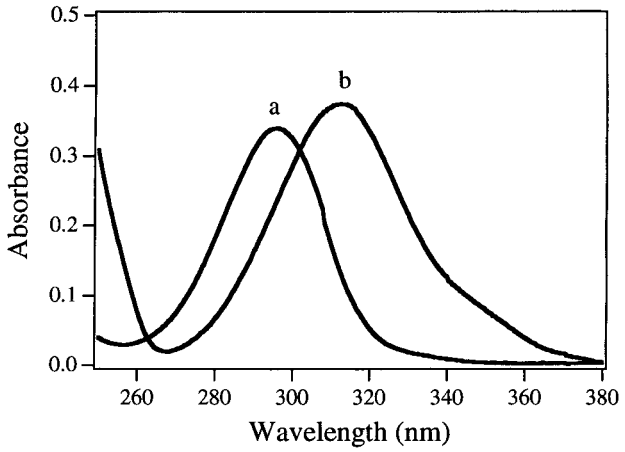

Figure 2. UV−vis absorption spectra of sodium salicylate (2×10^{-4} M) with (a) and without the presence of 8×10^{-3} M of $AlCl_3$ (b) in ethanol solution. Cell pathlength = 0.5 cm.

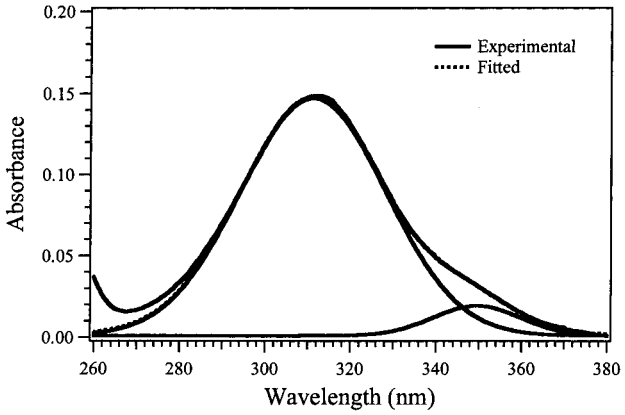

Figure 3. Deconvolution into Gaussian bands of the absorption spectrum of sodium salicylate (4×10^{-5} M) in the presence of $AlCl_3$ (1.3×10^{-3} M) in ethanol solution at 288 K

absorption maxima located at 311 and 346 nm, respectively (Figure 3). Absorption spectra recorded at lower temperatures show that the relative intensity of the band at 346 nm increases as the temperature decreases from room temperature to 160 K, the glass transition temperature of ethanol, below which the spectral changes suddenly cease. Part of the absorption spectra recorded from 288 to 105 K, corrected for thermal contraction of the solution, are shown in Figure 4. Below 160 K, all the spectra are superimposed in the figure and appear as a single trace. The isosbestic point observed at 328 nm clearly indicates an equilibrium between two interconverting species with distinct absorption bands. This conversion involves atomic motion, i.e., changes in bond length, bond angle, or bond rotation, that cease below the glass transition temperature, T_g.

Using Gaussian absorption profiles for both species, all of the absorption spectra can be deconvoluted into two separated bands; one located at 311 nm and the other located at 346 nm. Since the molar absorptivities for both species are the same at the isosbestic point, the molar absorptivities of the two species at the spectral maxima were calculated from the relative absorbances of the two species at their absorption maxima.[30] The spectral maximum molar absorptivities calculated by this procedure for the temperature-dependent spectra are 3400 and 10 000 (cm^{-1} dm mol^{-1}) for the species absorbing at the shorter (311 nm) and longer wavelength (346 nm), respectively. The estimated errors are ±500. From the absorbances of each species obtained from deconvoluted spectra at each temperature and the corresponding molar absorptivity, the concentration of each

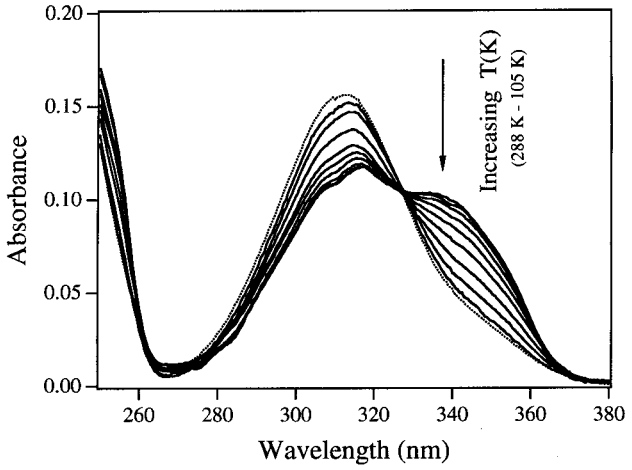

Figure 4. Absorption spectra of sodium salicylate (8×10^{-5} M) in the presence of $AlCl_3$ (6.5×10^{-4} M) in ethanol solution as a function of absolute temperature. Cell pathlength = 0.5 cm. Please note that all spectra below 160 K are superimposed and appear as a single trace.

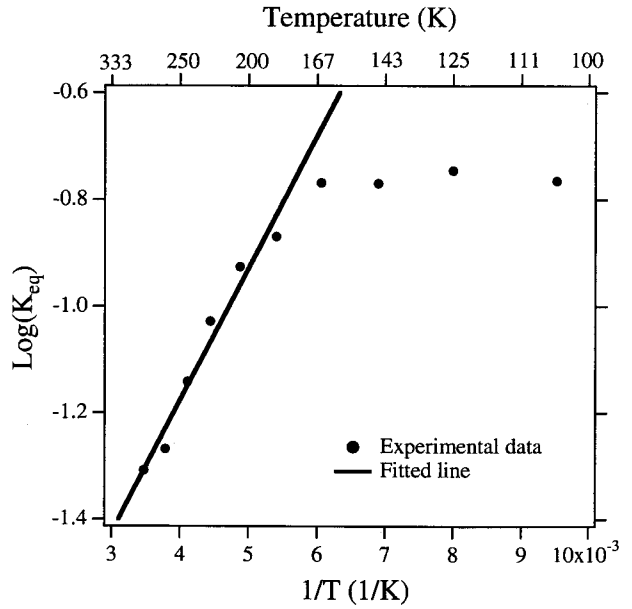

Figure 5. Plot of $\log(K_{eq})$ as a function of $1/T$ for the solution of sodium salicylate (8×10^{-5} M) in the presence of $AlCl_3$ (6.5×10^{-4} M) in ethanol. After 160 K, $\log(K_{eq})$ reaches a plateau. K_{eq} is equivalent to K_T defined in eq 3.

species, $[S_{311\ nm}]$ and $[S_{346\ nm}]$, at different temperatures were calculated using Beer's law. The temperature-dependent equilibrium concentration ratio, K_T, defined as

$$K_T = [S_{346\ nm}]/[S_{311\ nm}] \tag{3}$$

was calculated from the concentrations of each species and are plotted as a function of reciprocal absolute temperature, a van't Hoff plot, in Figure 5.

In the van't Hoff plot,

$$\log(K_T) = -\frac{\Delta H}{2.303RT} + \frac{\Delta S}{2.303R} \tag{4}$$

For the interconversion reaction

$$S_{311nm} \underset{K_r}{\rightleftharpoons} S_{346nm} \tag{5}$$

a plot of $\log(K_T)$ as a function of $1/T$ results in a straight line with a slope of $-\Delta H/2.303R$ and an intercept $\Delta S/2.303R$, where R is the gas constant. Figure 5 shows that above an absolute temperature of 160 K, the plot of $\log(K_T)$ vs $1/T$ is a straight line. From the slope and intercept the calculated enthalpy change is -1.13 kcal mol^{-1} and the entropy change is -9.92 cal mol^{-1} K^{-1}.

In the previous work it was found that sodium salicylate showed two distinctive absorption bands at 296 and 325 nm, respectively, with an isosbestic point at 310 nm.[30] The variation of absorption and excitation spectra as a function of temperature, fluorescence spectra, fluorescence lifetime, and fluorescence anisotropy data all pointed to the existence of salicylate in acetonitrile solvent as both the normal form (**B1**) and the tautomer (**B4**−**B6**) at equilibrium. The conversion reaction N ↔ T was found to be slightly endothermic with a small positive entropy change (0.97 cal mol^{-1}). Clearly, there are significant differences for both ΔH and ΔS between Al(III)−salicylate complexes and sodium salicylate. These differences likely reflect the different nature of interaction between salicylate and either the aluminum or sodium cations. The current results for the Al(III)−salicylate complex system in ethanol also indicate the presence of two species in equilibrium, with the absorption maximum of the second species red-shifted 35 nm relative to the main species. From the similarity of the spectral changes between the Al(III)−salicylate system and that of the sodium salicylate system, absorption and fluorescence spectra, fluorescence lifetime, and the anisotropy data to be presented hereafter, we assign the 311 nm absorption to the normal form of the Al(III) salicylate complex in which Al(III) binds to the carboxylate group (**C1**), preserving the hydrogen bond between the phenol group and the carbonyl oxygen, and the 346 nm absorption to a tautomer form of the Al(III)−salicylate complex in which Al(III) binds to the phenoxide oxygen (**C6**). The fact that the interconversion reaction stops below the glass temperature indicates that the reaction involves large-amplitude nuclear motion, i.e., an atomic rearrangement which we hypothesize to be the exchange of Al(III) between the carboxylate and the phenolate groups.

It is known that for a given polyprotic acid, the acid dissociation constants vary significantly in different solvents.[54] Both the dielectric constant and the solvating power for the separated ions affect a solvent's ionizing ability. Because of dielectric shielding, the attractive force between oppositely charged ions is inversely proportional to the dielectric constant. The solvating power is determined by the stability of the solvated ions. Solvation of carboxylic acids is dominated by dielectric shielding of the separated ions.[54,55] According to Bos and Dahmen,[56] acid dissociation is greatly hindered in solvents of smaller dielectric constant. Even in a strong base such as pyridine, the basicity of the solvent cannot compensate for the effect of its small dielectric constant limiting the extent of acid dissociation. For example, in water ($\epsilon = 78.3$) the pK_a of benzoic acid is 3.99 but in pyridine ($\epsilon = 12.3$), the pK_a is 11, seven units larger than in water. In a protic solvent like EtOH ($\epsilon = 24.3$), the pK_a of benzoic acid is still high (10.25).[56] A general trend is that the larger the pK_a is in water, the more the pK_a is increased when the acid is in a solvent of low dielectric constant, i.e., the more sensitive the pK_a is to lowered dielectric constant.

The phenol proton pK_a of salicylate (pK_{a2}) is 13.5 in aqueous solution. From the trend of pK_a change vs solvent dielectric constant, the pK_{a2} will be expected to be tens of units larger in ethanol. This excludes any possibility of formation of the phenolate anion (Sal^{2-}). As evidenced from the fluorescence emission spectra (next section), formation of a bidentate chelate

TABLE 1: Characteristics of Methyl Salicylate Derivatives

solution	absorption maximum (nm)	emission maximum (nm)
methyl salicylate in cyclohexane	308	339, 441
methyl salicylate in ethanol	307	350, 438
methyl salicylate in water at pH 6	304	360, 420
methyl salicylate at pH 12	334	395
sodium salicylate in water at pH 6	296	415
sodium salicylate in water at pH 1	304	436
salicylic acid in ethanol	305	415[a]
anisic acid in ethanol	293	352
anisic acid in water at pH 1.0	296	—[b]
anisic acid in water at pH 6	279	

[a] The spectral maximum of the weak emission is masked by the emission from the salicylate anion. [b] The weak emission is masked by more intense emission from either anisate or other impurities.

between Al(III) and salicylate, in which both the carboxylate oxygen and the phenol oxygen bind to Al(III), can be excluded in ethanol solution even though the bidentate complex is the major component in aqueous solution.[57] Therefore we conclude that the Al(III)−salicylate complexes in equilibrium in ethanol are the monodentate species described above (**C1, C6**, and their rotamers and/or resonance forms). In other words, the phenolic proton and the carboxylate Al(III) may exchange their binding positions (**C1** and **C6**), but the proton does not dissociate from the Al(III)−salicylate complex.

To elucidate the structures of the Al(III)−salicylate complexes in ethanol, absorption spectra of methyl salicylate and *o*-anisic acid were recorded under different pH conditions. Anisic acid and methyl salicylate are both ortho-substituted benzene derivatives with structures similar to that of salicylic acid. From an experimental point of view, anisic acid and methyl salicylate provide models of the effect of carboxylic acid and phenol proton dissociation on the absorption spectra. The pK_a of aqueous anisic acid is 4.09.[38] There is no reported pK_a value for methyl salicylate. As an ortho-substituted phenol with a weak hydrogen bond between the phenol group and the methoxy oxygen, methyl salicylate pK_a is expected to be similar to that of *o*-methoxy phenol (pK_a = 9.98).[38] Therefore, at pH 6 anisic acid exists mainly as the anisate anion while methyl salicylate will be mostly in phenolate form at pH 12.5. The spectral absorption maxima of anisic acid at pH 1 and pH 6, salicylic acid at pH 1 and pH 6, and methyl salicylate at pH 6 and pH 12.5, are listed in Table 1. Data in Table 1 indicate that dissociation of the anisic acid carboxylic acid proton causes a spectral blue-shift of ~17 nm. This is similar to the trend in salicylic acid in which dissociation shifts the absorption maxima from 307 nm (salicylic acid) to 297 nm (salicylate anion). In contrast, for methyl salicylate the absorption spectra show a large red-shift from 304 to 334 nm upon dissociation of the phenol proton at pH 12. The spectral shift of methyl salicylate upon phenol proton dissociation confirms that the phenolate form of the salicylate anion absorbs and emits at longer wavelength relative to its carboxylate form. This is consistent with contributions from the quinoidal and Zwitter ion resonance structures to the phenolate electronic structure (**B4**−**B6**). Gas-phase ab initio calculations appear to confirm the relative energetics presented here. However, without the inclusion of explicit solvent molecules to stabilize the Al^{3+} ion, the relative energies are strongly overestimated.[58]

Fluorescence Excitation and Emission Spectra. Fluorescence excitation and emission spectra were recorded for sodium salicylate alone and sodium salicylate in the presence of excess $AlCl_3$ at room temperature and 105 K in ethanol solution

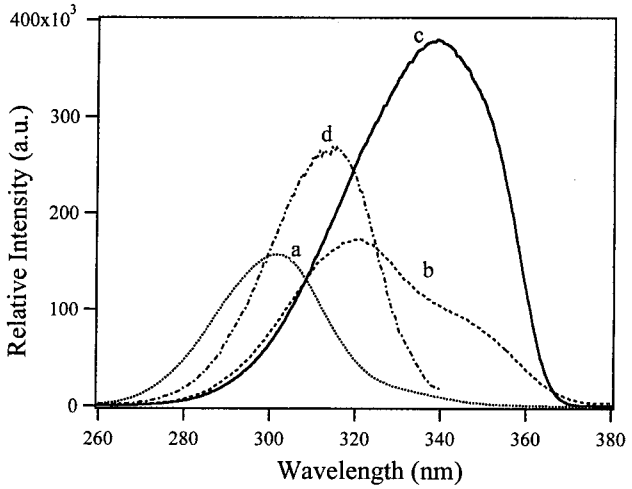

Figure 6. Fluorescence excitation spectra of sodium salicylate (2.4×10^{-5} M) only (a) and in the presence of 8×10^{-4} M of $AlCl_3$ (b−d) in ethanol solution. In (a) λ_{em} = 415 nm, T = 298 K; in (b) λ_{em} = 409 nm, T = 298 K; in (c) λ_{em} = 409 nm, T = 105 K; and in (d) λ_{em} = 350 nm, T = 105 K, and the intensity was multiplied by a factor of 10.

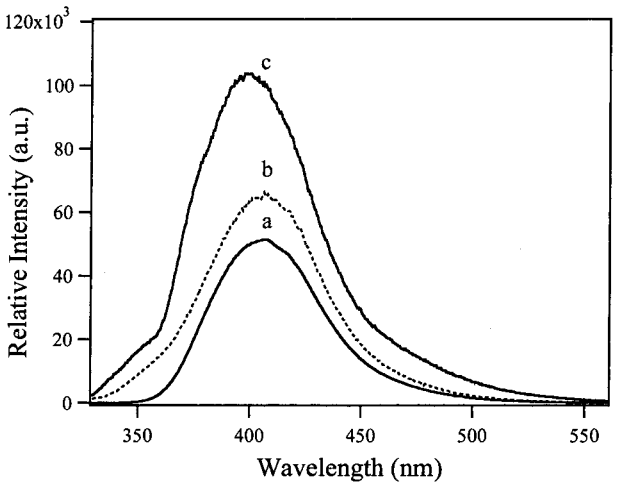

Figure 7. Fluorescence emission spectra of sodium salicylate (2.4×10^{-5} M) only (a) and in the presence of 8×10^{-4} M of $AlCl_3$ (b and c) in ethanol solution. In (a) λ_{ex} = 300 nm, T = 298 K; in (b) λ_{ex} = 309 nm, T = 298 K; in (c) λ_{ex} = 309 nm, T = 105 K.

(Figures 6−8). The excitation spectra (Figure 6) generally resemble those of the absorption spectra (Figure 2) except that the apparent excitation maximum of the Al(III)−salicylate solution is somewhat red-shifted due to a larger intensity contribution from the longer wavelength band at 346 nm, implying a larger quantum yield for the latter. The 346 nm band increases appreciably as temperature is lowered, consistent with the change of absorption spectra at different temperatures (Figure 4). Excitation spectra recorded at different emission wavelengths (409 and 360 nm, respectively, Figure 6) indicate that fluorescence of the major emission band in the spectral region from 380 to 450 nm originates from excitation of both the 311 nm band and 346 nm band while the short wavelength emission band at 360 nm derives solely from excitation in the 311 nm band.

Fluorescence emission spectra of the Al(III)−salicylate complexes show a spectral maximum at around 405 nm, slightly blue-shifted relative to that of sodium salicylate (415 nm). A short wavelength shoulder (~360 nm) appears when the excitation wavelength is within the 311 nm absorption band (Figure 7a,b). This shoulder band becomes better resolved in

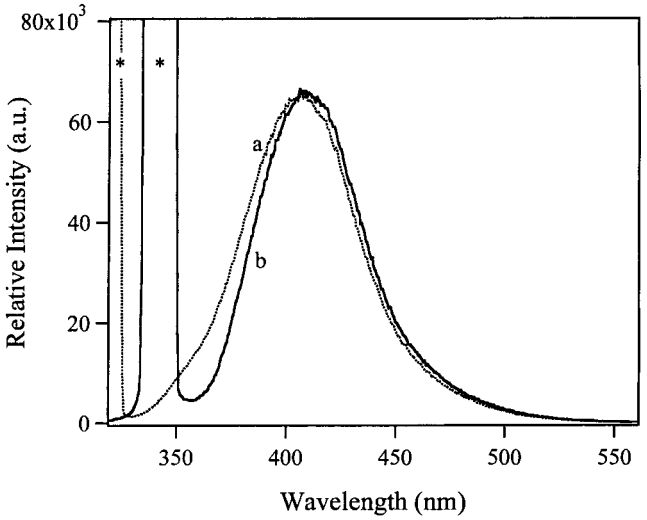

Figure 8. Fluorescence emission spectra of salicylate (2.4×10^{-5} M) in the presence of 8×10^{-4} M of $AlCl_3$ in ethanol solution. In (a) λ_{ex} = 300 nm, T = 298 K; in (b) λ_{ex}= 309 nm, T = 298 K. The asterisk denotes Rayleigh scattering. The spectra are normalized to the same peak intensity.

ethanol glass at 105 K (Figure 7c). At 105 K there also appears to be a weak emission band at much longer wavelength (~480 nm).

Emission spectra excited in the 346 nm band are slightly red-shifted relative to emission spectra excited at 311 nm (Figure 8a,b). While the lower relative emission intensity of trace b (Figure 8) at wavelengths ≤420 nm (λ_{ex} = 346 nm) might be attributed to the lack of contribution from the short wavelength shoulder which appears only when excited at the 311 nm band, the constantly higher emission intensity at wavelengths ≥420 nm suggests that excitation in the two absorption bands yields two different emission spectra.

Figures 6 and 7 indicate that the dominant complex between Al(III) and salicylate in ethanol solution has an absorption maximum of 311 nm and emission maximum of 405 nm. The large Stokes gap (7500 cm^{-1}) between the first excited state and the ground state is similar to that of other salicylate derivatives[24−26] and is a consequence of ESIPT.[24−28] For ESIPT-type emission to occur, the phenol group must be preserved in the molecule with an IHB between the phenol group and the carbonyl oxygen. These characteristics point to a monodentate complex in which Al(III) binds to the carboxylate group of the normal form of salicylate (**C1**). In the excited state the phenol oxygen becomes more acidic and the carbonyl oxygen becomes more basic, and proton transfer from the phenol oxygen to the carbonyl oxygen occurs, resulting in a large Stokes shift of the fluorescence emission.

The short wavelength emission band at 360 nm only appears upon excitation at the 311 nm absorption band of Al(III)−salicylate complexes. This type of localized UV emission (Stokes gap ≤ 5000 cm^{-1}) has been observed for several other methyl salicylate derivatives and was assigned previously either to the closed form II (**A2**) with an IHB between the phenol group and the methoxy oxygen for methyl salicylate or to the open form (**A3**) for salicyl aldehyde and amides.[1−12] For Al(III)−salicylate complexes both types of structures are possible (**C2, C3**). Since repulsion between Al(III) and the phenol proton is expected to make the complex **C2** less stable, we assign the localized emission at 360 nm to the open form Al(III)−salicylate complex (**C3**).

As shown in Figure 4, the Al(III)−salicylate complex that absorbs at 346 nm is in equilibrium with the complexes in which salicylate exists in its normal form (**C1**). A similar equilibrium has been observed for the salicylate anion in polar nonprotic solvent.[30] The red-shift of the absorption band suggests that in this complex tautomerization of salicylate has occurred. For sodium salicylate, excitation at either absorption band of the salicylate anion (**B1** or **B4**) results in the same emission spectrum, indicating that in the excited state the normal form of salicylate converts into the excited state of the tautomer from which emission occurs.[30] However, as seen in Figure 8, the excited state of the tautomeric Al(III)−salicylate complex absorbing at 346 nm may be different from the metastable excited state generated through the ESIPT process via the normal form of salicylate absorbing at 311 nm. The cause of such a difference lies in the fact that there are several resonance forms for the salicylate tautomer (**B4**−**B6**). The Al(III) ion may bind to tautomeric salicylate through either the carboxylate oxygen (**C4, C5**) or the phenolate oxygen (**C6**). Structurally, both **C4** and **C5** closely resemble that of the normal form Al(III)−salicylate complex (**C1**) in the excited state after the ESIPT process. However, in the tautomer (**C6**), Al(III) binds to the phenolate oxygen. Because of the 3+ charge on the Al(III) cation, it is expected that the electronic structure of **C6** may be significantly different from the complex derived from the other two resonance forms (**B4, B5**) as well as the normal form complex (**C1**). The difference will affect the characteristics of their fluorescence emission. The small difference between the fluorescence emission spectra obtained upon excitation at 311 and 346 nm (Figure 8) as well as the considerably different fluorescence lifetimes (next section) indicate that structure **C6** is the most stable of the three Al(III)−salicylate isomers. No evidence of significant contributions of either **C4** or **C5** is available in the present study. It is therefore possible that the small difference between the emission spectra of the normal form and the tautomer form of Al(III)−salicylate complexes (Figure 8) is coincidental.

To test this hypothesis, absorption, excitation, and emission spectra of the complexes of another trivalent cation, La(III), with salicylate in ethanol were recorded. Both the absorption (not shown) and excitation spectra (Figure 9 panel A) of La(III)−salicylate complexes are similar to those of Al(III)−salicylate (Figure 6). However, the emission spectra (Figure 9 panel B) demonstrate significant differences upon excitation into the absorption band of the normal form (λ_{ex} = 300 nm) or the tautomer form of the La(III)−salicylate complex (λ_{ex} = 345 nm). Excitation at 300 nm leads to a largely Stokes-shifted emission spectra with maximum at 421 nm but excitation at 345 nm leads to shorter wavelength emission at 409 nm. La(III) forms inner sphere complexes with salicylate similar to Al(III).[59] Upon complexation, Al(III) is expected to have a similar effect on the spectra of salicylate as La(III). Therefore, the slight differences shown in Figure 8 may indeed be due to a coincidental overlap of the spectra.

The weak emission band at 480 nm (Figures 7 and 8) that only appears at low temperatures could not be resolved from the main emission band due to its low intensity. However, fluorescence lifetime measurements at 77 K indicate that its emission lifetime was on the order of tens of μs. We attribute this long-lived emission to phosphorescence from the Al(III)−salicylate complexes. Phosphorescence is quenched in room-temperature solutions by many fast nonradiative deactivation processes that deplete the population of excited triplet states.[60]

Fluorescence Decay and Anisotropy Characteristics. Fluorescence lifetimes were recorded at a combination of excitation wavelengths of 300 and 335 nm, and emission wavelengths of

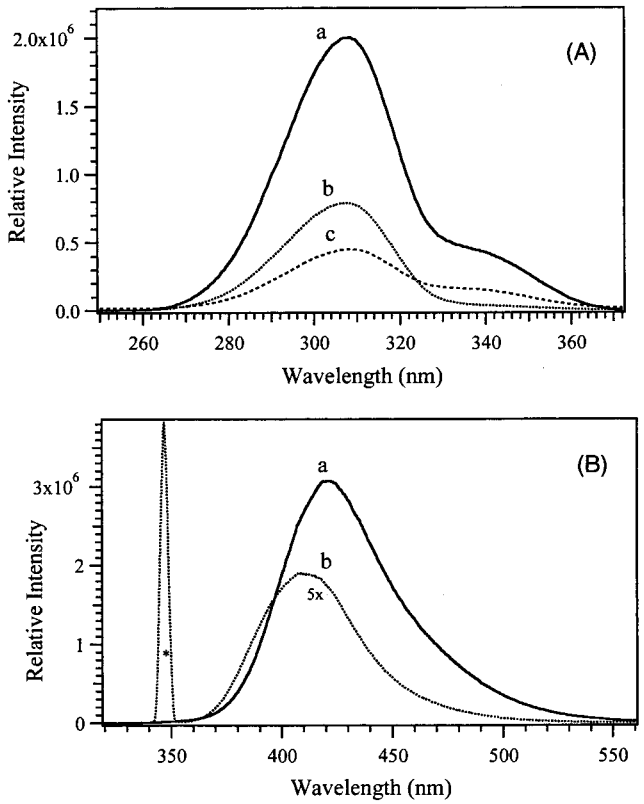

Figure 9. Fluorescence excitation spectra (A) and emission spectra (B) of La(III)−salicylate in ethanol. [La(III)] = 1×10^{-2} M, [Sal] = 1×10^{-4} M. In (A): a, $\lambda_{em} = 410$ nm; b, $\lambda_{em} = 480$ nm; c, $\lambda_{em} = 385$ nm. In (B): a, $\lambda_{ex} = 300$ nm; b, $\lambda_{ex} = 345$ nm. Trace b was multiplied by a factor of 5 for clarity. The asterisk denotes Rayleigh scattering.

360, 410, 450, and 480 nm at room temperature. Excitation at 300 nm results in double exponential fluorescence decays at shorter emission wavelengths ($\lambda_{em} \leq 410$ nm) with lifetimes of 2.2 and 6.5 ns and single exponential decays (6.5 ns) at longer wavelengths. Excitation at 335 nm leads to double exponential decays with lifetimes of 2.2 ns and 8.2 ns in the short emission wavelength region ($\lambda_{em} \leq 410$ nm) and a single exponential decay (of 8.2 ns) only at the longer emission wavelengths. From Figure 3 it is known that the normal form Al(III)−salicylate complexes, including both the closed form and the open form, are excited at both 300 and 335 nm. Therefore, the 2.2 ns lifetime at shorter emission wavelength can be attributed to the open form complex (**C3**). Shorter fluorescence lifetimes of the open form salicyl derivatives has also been observed by other authors.[23−25] Accordingly, the 6.5 ns lifetime is associated with the normal form of the Al(III)−salicylate complex (**C1**) while the 8.2 ns lifetime is associated with the phenolate-type Al(III)-salicylate complex (**C6**). The different fluorescence lifetimes again confirm that two isomers coexist with distinct ground and excited states and that in the tautomeric Al(III)−salicylate complex, Al(III) binds to the tautomer form of salicylate anion through the phenolate oxygen.

Polarized emission spectra were recorded for Al(III)−salicylate complexes in ethanol at room temperature and in ethanol glass at 105 K using vertically polarized excitation. The steady-state fluorescence anisotropies were calculated using eqs 1 and 2. At room temperature, excitation in either band results in nearly zero anisotropy (Figure 10a) as expected since the fluorescence lifetime is more than 2 orders of magnitude longer than the rotational diffusion time of the molecules (∼20 ps), so that the orientation of the excited molecules is totally randomized during the excited-state lifetime.[27] However, in ethanol glass

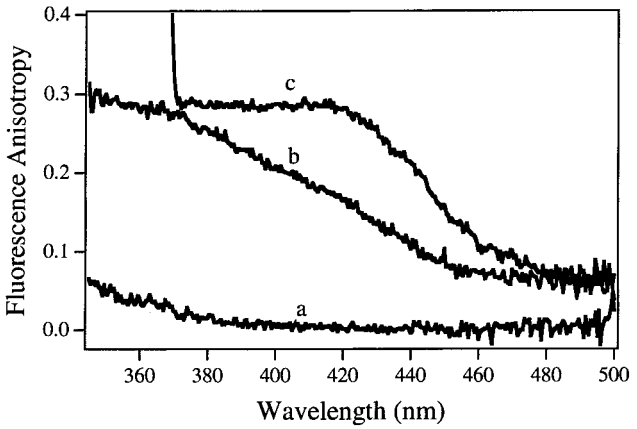

Figure 10. Steady-state fluorescence anisotropies of sodium salicylate (2.4×10^{-5} M) only (a) and in the presence of 8×10^{-4} M of $AlCl_3$ (b and c) in ethanol solution. In (a) $\lambda_{ex} = 360$ nm, $T = 298$ K; in (b) $\lambda_{ex} = 309$ nm, $T = 105$ K; in (c) $\lambda_{ex} = 360$ nm, $T = 105$ K.

at 105 K, the anisotropies are much higher and vary with excitation wavelength (Figure 10b,c). When excited at 360 nm, the emission anisotropy is high (∼0.3) from 370 to 420 nm and then decreases rather sharply from 420 to 460 nm, reaching ∼0.07 at 500 nm (Figure 10c). However, when excited at 309 nm, anisotropy is large only from 340 to 370 nm and then decreases gradually reaching ∼0.07 at 480 nm (Figure 10b). These observations are different from those for sodium salicylate in ethanol glass in which the anisotropies are large and constant throughout the entire emission range when excited in either absorption band.[27]

The large anisotropy from 370 to 420 nm for excitation at 360 nm indicates that the directions of the absorption and emission transition-dipole moments are nearly parallel for the proton-transferred Al(III)−salicylate complex (**C4**). This is similar to sodium salicylate. This is also true for the open form of the proton-not-yet-transferred Al(III)−salicylate complex (**C3**) which has large emission anisotropy from 340 to 380 nm when excited at 309 nm. However, in contrast with sodium salicylate, the decreasing anisotropy from 380 to 430 nm while excited at 309 nm suggests that the absorption dipole moment of the proton-not-yet-transferred Al(III)−salicylate complex (**C1**−**C3**) and the emission dipole moment of the proton-transferred Al(III)−salicylate complex are no longer parallel. Because of the large positive charge on the aluminum cation, ESIPT involves significant electronic redistribution from the proton-not-yet-transferred excited state (e.g., **C1***) to the proton-transferred excited state (**C4***). Direct consequences of such an electronic redistribution are a noticeable change of bond lengths as well as large scale atomic motion of the aluminum and proton. These observations are consistent with the temperature dependence of the normal to tautomer equilibrium for Al(III)−salicylate complexes (Figure 4).

Triplet state emission anisotropy of aromatic molecules excited via singlet state absorption should reach −0.2 since the direction of the phosphorescence transition dipole moment is perpendicular to the molecular plane and therefore also perpendicular to the singlet excitation dipole moment.[43] The small anisotropy and long emission time for the band around 480 nm confirms the phosphorescence nature of this band. The measured anisotropy is greater than −0.2 due to spectral overlap of fluorescence and phosphorescence in that wavelength range. For sodium salicylate no phosphorescence emission is observed, indicating that the triplet state energy is much lower than the singlet excited state and/or undergoes rapid nonradiative decay

to the ground state. A search at longer wavelengths failed to detect any long-lived, low anisotropy emission that would be characteristic of salicylate anion phosphorescence. The phenolic proton may provide the vibrational coupling needed for efficient nonradiative decay of the lowest salicylate triplet state. By contrast, in the phenolate Al(III)−salicylate complex, rapid return of the proton to the phenoxy oxygen is inhibited, enabling phosphorescence characteristic of a substituted benzoic acid.

The results shown above demonstrate that the ESIPT fluorescence characteristics of salicylate can serve as a spectral probe for the investigation of the structure and bonding of salicylate complexes with metal ions. For sodium salicylate the normal forms (**B1**−**B3)** and the tautomer forms (**B4**−**B6**) display identical fluorescence emission spectra, lifetimes, and anisotropies. This implies the sodium cation only interacts with carboxylate anions in an electrostatic and most likely outer-sphere manner, in which Na(I) and the salicylate anion are separated by multiple solvent molecules, forming outer-sphere complexes. Replacement of sodium with the trivalent cations Al(III) or La(III) causes the distinction between the emission spectra of the normal form (**C1**) and tautomer form (**C6**) of the metal−salicylate complex due to the nature of inner-sphere complexation in which the metal cation directly binds to an oxygen of the salicylate anion. Therefore, the tautomeric Al(III)−salicylate complex in which Al(III) binds to the phenolate oxygen (**C6**) is more favored than normal Al(III)−salicylate complexes in which Al(III) binds to the carboxylate oxygen (**C1**−**C3**) of the salicylate anion.

IV. Conclusions

In the previous paper we reported the presence of a ground-state proton-transferred tautomer of salicylate in acetonitrile.[30] The presence of this tautomer is barely noticeable in ethanol solutions. In this paper we have demonstrated that the presence of a highly charged cation, Al(III), further stabilizes the tautomer form of salicylate. The presence of rotameric isomers and different resonance forms of the tautomers offers several binding sites for complexation between Al(III) and salicylate. UV−visible absorption spectroscopy, fluorescence spectroscopy and anisotropy, and fluorescence lifetime data all indicate that three ground-state Al(III)−salicylate complexes form in ethanol solution, all with monodentate binding characteristics. In complex types I and II, salicylate binds to Al(III) through the carboxylate group (**C1** and **C3**) and in type III, salicylate binds to Al(III) through the phenolate oxygen in which salicylate exists in its proton transferred tautomer form (**C6**). The difference between type I and II is that in the former the phenol group forms a hydrogen bond with the carbonyl group while in the latter the phenol proton is turned away from the carbonyl oxygen. Absorption spectra recorded at temperatures between 105 and 298 K indicate that type I and II complexes convert to type III complexes as the temperature is lowered. At the glass transition temperature of ethanol the conversion ceases, indicating large amplitude atomic motion is involved in the equilibrium.

Acknowledgment. This research was supported by the Molecular Science Research Initiative at the Pacific Northwest National Laboratory (PNNL) and performed at the W. R. Wiley Environmental Molecular Sciences Laboratory, a national scientific user facility sponsored by the Department of Energy's Office of Biological and Environmental Research and located at PNNL. Pacific Northwest National Laboratory is operated for the U.S. Department of Energy by Battelle under Contract DE-AC06-76RLO 1830.

References and Notes

(1) Barbara, P. F.; Walker, G. C.; Smith, T. P. *Science* **1992**, *256*, 975.
(2) Barbara, P. F.; Walsh, P. K.; Brus, L. E. *J. Phys. Chem.* **1989**, *93*, 29.
(3) Berlman, I. B. *Handbook of Fluorescence Spectra of Aromatic Molecules*, 2nd ed.; Academic Press: New York, 1997; Graph 34A, p 166.
(4) Bisht, P. B.; Okamoto, M.; Hirayama, S. *J. Phys. Chem.* **1997**, *101*, 8850−8855.
(5) Bisht, P. B.; Petek, H.; Yoshihara, K.; Nagashima, U. *J. Chem. Phys.* **1995**, *103*, 5290−5306.
(6) Bureiko, S. F.; Oktiabr'sky, V. P. *J. Mol. Struct.* **1995**, *349*, 53−56.
(7) Estevez, C. M.; Rios, M. A.; Rodriguez, J. *Struct. Chem.* **1992**, *3*, 381−387.
(8) Kubicki, J. D.; Itoh, M. J.; Schroeter, L. M.; Apitz, S. E. *Environ. Sci. Technol.* **1997**, *31*, 1151−1156.
(9) Formosinho, S. J.; Arnaut, L. G. *J. Photochem. Photobiol. A: Chem.* **1993**, *75*, 21−48.
(10) Goodman, J.; Brus, L. E. *J. Am. Chem. Soc.* **1978**, *100*, 7472.
(11) Gormin, D.; Kasha, M. *Chem. Phys. Lett.* **1988**, *153*, 574−576.
(12) Heldt, J.; Gormin, D.; Kasha, M. *Chem. Phys.* **1989**, *136*, 321−334.
(13) Helmbrook, L.; Kenny, J. E.; Kohler, B. E.; Scott, G. W. *J. Phys. Chem.* **1983**, *87*, 280.
(14) Hoshimoto, E.; Yamauchi, S.; Hirota, N.; Nagaoka, S. *J. Phys. Chem.* **1991**, *95*, 10229−10235.
(15) Joshi, H C.; Mishra, H.; Tripathi, H. B. *J. Photochem. Photobiol., A, Chemistry* **1997**, *105*, 15.
(16) Lahmani, F.; Zehnacker-Rentien, A. *J. Phys. Chem. A* **1997**, *101*, 6141−6147.
(17) Lakowicz, J. R. *Principles of Fluorescence Spectroscopy*; Plenum Press: New York, 1983; Vol. 5, pp 111−153.
(18) Law, K.-Y.; Shoham, J. *J. Phys. Chem.* **1994**, *98*, 3114−3120.
(19) Morgan, M. A.; Orton, E.; Pimentel, G. C. *J. Phys. Chem.* **1990,** *94*, 7927.
(20) Nagaoka, S.; Nagashima, U. *Chem. Phys.* **1989**, *136*, 153−163.
(21) Nagaoka, S.; Nagashima, U.; Ohta, N.; Fujita, M.; Takemura, T. *J. Phys. Chem.* **1988**, *92*, 166−171.
(22) Nagy, P. I.; Dunn, W. J., III; Alagona, G.; Ghio, C. *J. Phys. Chem.* **1993**, *97* (46), 28−42.
(23) Orton, E.; Morgan, M. A.; Pimentel, G. A. *J. Phys. Chem.* **1990**, *94*, 7936.
(24) Sanchez-Cabezudo, M.; De Paz, J. L. G.; Catalan, J.; Amat-Guerri, F. *J. Mol. Struct.* **1985**, *131*, 277−289.
(25) Sundaralingam, M.; Jensen, L. H. *Acta Cryst.* **1965**, *18*, 1053−1058.
(26) Vener, M. V.; Scheiner, S. *J. Phys. Chem.* **1995**, *99*, 642−649.
(27) Weller, A. *Prog. React. Kinet.* **1961,** *1*, 188.
(28) Zuccarello, F.; Buemi, G. *Gazz. Chim. Ital.* **1988**, *118*, 359−363.
(29) Sharpley, W. A.; Backkay, G. B.; Warr, G. G. *J. Phys. Chem.* **1998**, *102*, 1938−1944.
(30) Friedrich, D. M.; Wang, Z.; Joly, A. G.; Peterson, K. A.; Callis, P. R. *J. Phys. Chem.* **1999**, *103*, 9644−9653.
(31) Ainsworth, C. C.; Fredrickson, J. K.; Smith, S. C. *Sorption and Degradation of Pesticides and Organic Chemicals in Soils*; Linn, D. M., Ed.; SSSA Special Pub. No. 32: Madison, WI, 1993; pp 125−144.
(32) Ainsworth, C. C.; McVeety, B. D.; Smith, S. C.; Zachara J. M. *Clays Clay Miner.* **1991**, *39*, 416.
(33) Biber, M.; Stumm, W. *Geochim. Cosmochim. Acta* **1994**, *58*, 1999.
(34) Hendershot, W. H.; Courchesne, F.; Jeffries, D. S. *The Environmental Chemistry of Aluminum*, 2nd ed.; Sposito, G., Ed.; CRC Press: Boca Raton, FL, 1996; pp 419−449.
(35) Drever, J. I.; Stillings, L. L. *Colloids Surf.* **1997**, *120*, 167.
(36) Furrer, G.; Stumm, W. *Geochim. Cosmochim. Acta* **1986**, *50*, 1947.
(37) Stevenson, F. J. *Humus Chemistry; Genesis, Composition, Reactions*, 2nd ed.; Wiley-Interscience: New York, 1994.
(38) Martell, A. E.; Smith, R. M. *Critical Stability Constants: Other Organic Ligands*; Plenum Press: New York, 1977.
(39) Amrhein, C.; Suarez, D. L. *Geochim. Cosmochim. Acta* **1988**, *52*, 2785.
(40) Ohman, L. O.; Sjoberg, S. *Acta Chim. Scand.* **1983**, *A37*, 875.
(41) Secco, F.; Venturini, M. *Inorg. Chem.* **1975**, *14*, 1978.
(42) Perlmutter-Hayman, B.; Tapuhi, E. *Inorg. Chem.* **1978**, *18*, 875.
(43) Campbell, P. G. C.; Bisson, M.; Bougie, R.; Tessier, A.; Villeneuve, J. P. *Anal. Chem.* **1983**, *55*, 2246.
(44) Taylor, T. A.; Patterson, H. A.; Cronan, C. S.; Schofield, C. A. *Anal. Chim. Acta* **1993**, *278*, 259.
(45) Parfitt, R. L.; Framer, V. C.; Russell, J. D. *J. Soil Sci.* **1977**, *28*, 29.
(46) Yost, E. C.; Tejedor-Tejedor, M. I.; Anderson, M. A. *Environ. Sci. Technol.* **1990**, *24*, 822.

(47) Kung, K. H.; McBride, M. B. *Clays Clay Miner.* **1989**, *37*, 333.
(48) Thomas, F.; Masion, A.; Bottero, J. Y.; Rouiller, J.; Montigny, F.; Genevrier, F. *Environ. Sci. Technol.* **1993**, *27*, 2511.
(49) Thomas, F.; Masion, A.; Bottero, J. Y.; Rouiller, J.; Genevrier, F.; Boudot, D. *Environ. Sci. Technol.* **1991**, *25*, 1553.
(50) Casey, W. H.; Phillips, B. L.; Nordin, J. P.; Sullivan, D. J. *Geochim. Cosmochim. Acta* **1997**, *62*, 2789.
(51) Motekaitis, R. J.; Martell, A. E. *Inorg. Chem.* **1984**, *23*, 18.
(52) Friedrich, D. M..; Mathies, R.; Albrecht, A. C. *J. Mol. Spectrosc.* **1974**, *51*, 166.
(53) Holtom, G. R. *SPIE* **1990**, *1204*.
(54) Stewart, R. *The Proton: Applications To Organic Chemistry*; Academic Press: New York, 1985; p 29.
(55) Grunwald, E.; Berkowitz, B. J. *J. Am. Chem Soc.* **1951**, *73*, 4939.
(56) Bos, M.; Dahmen, E. A. M. F. *Anal. Chim. Acta* **1971**, *55*, 285.
(57) Ainsworth, C. C.; Friedrich, D. M.; Gassman, P. L.; Wang, Z.; Joly, A. G. *Geochim. Cosmochim. Acta* **1998**, *62*, 595.
(58) Peterson, K. A. Private communications.
(59) Moeller, T.; Martin, D. F.; Thompson, L. C.; Ferrus, F.; Feistel, G. R.; Randall, W. J. *Chem. Rev.* **1965**, *65*, 1.
(60) Birks, J. B. *Organic Molecular Photophysics*; John Wiley & Sons: New York, 1975; Vol. 2, pp 547−555.